Dissipative ring solitons with vorticity

J. M. Soto-Crespo[1], N. Akhmediev[2], C. Mejía-Cortés[1] and N. Devine[2]

[1]*Instituto de Óptica, C.S.I.C., Serrano 121, 28006 Madrid, Spain*
jsoto@io.cfmac.csic.es

[2]*Optical Sciences Group, Research School of Physical Sciences and Engineering, The Australian National University, Canberra ACT 0200, Australia*
nna124@rsphysse.anu.edu.au

Abstract: We study dissipative ring solitons with vorticity in the frame of the (2+1)-dimensional cubic-quintic complex Ginzburg-Landau equation. In dissipative media, radially symmetric ring structures with any vorticity m can be stable in a finite range of parameters. Beyond the region of stability, the solitons lose the radial symmetry but may remain stable, keeping the same value of the topological charge. We have found bifurcations into solitons with n-fold bending symmetry, with n independent on m. Solitons without circular symmetry can also display $(m+1)$-fold modulation behaviour. A sequence of bifurcations can transform the ring soliton into a pulsating or chaotic state which keeps the same value of the topological charge as the original ring.

OCIS codes: (190.3100) Instabilities and chaos; (190.6135) Spatial Solitons.

References and links

1. G. K. Batchelor, *An Introduction to Fluid Dynamics*, (Cambridge University Press, 1967).
2. H. Kleinert, Multivalued Fields in Condensed Matter, Electrodynamics, and Gravitation, (World Scientific, Singapore, 2008).
3. J. G. Cramer, R. L. Forward, M. S. Morris, M. Visser, G. Benford, and G. A. Landis, "Natural Wormholes as Gravitational Lenses," Phys. Rev. D51, 3117-3120 (1995).
4. V. Yu. Bazhenov, M. S. Soskin, and M. V. Vasnetsov, "Screw dislocations in light wavefronts," J. Mod. Opt. **39**, 985-990 (1992).
5. J. P. Torres, J. M. Soto-Crespo, L. Torner, and D. V. Petrov "Solitary-wave Vortices in Quadratic Nonlinear Media," J. Opt. Soc. Am. B **15**, 625-627 (1998).
6. A. Dreischuh, G. G. Paulus, F. Zacher, F. Grasbon and H. Walther, "Generation of multiple-charged optical vortex solitons in a saturable nonlinear medium," Phys. Rev. E **60**, 6111-6117 (1999).
7. N. K. Efremidis, K. Hizanidis, B. A. Malomed, and P. Di Trapani, "Three-Dimensional Vortex Solitons in Self-Defocusing Media," Phys. Rev. Lett. **98**, 113901 (2007).
8. B. A. Malomed, L.-C. Crasovan and D. Mihalache, "Stability of vortex solitons in the cubic-quintic model," Physica D **161**, 187-201 (2002).
9. Y. J. He, B. A. Malomed, D. Mihalache and H. Z. Wang, "Crescent vortex solitons in strongly nonlocal nonlinear media," Phys. Rev. A **78**, 023824 (2008).
10. D. N. Neshev, A. Dreischuh, V. Shvedov, A. S. Desyatnikov, W. Krolikowski, and Y. S. Kivshar, "Observation of polychromatic vortex solitons," Opt. Lett. **33**, 1851 (2008).
11. V. Tikhonenko, Y. Kivshar, V.V. Steblina, and A.A. Zozulya, "Vortex solitons in a saturable optical medium," J. Opt. Soc. Am. B **15**, 79-86 (1998).
12. Y. V. Kartashov, V. A. Vysloukh, and L. Torner, "Stable Ring-Profile Vortex Solitons in Bessel Optical Lattices," Phys. Rev. Lett. **94**, 043902 (2005).
13. J. Wang and J. Yang, "Families of vortex solitons in periodic media," Phys. Rev. A **77**, 033834 (2008).
14. J. Yang, "Stability of vortex solitons in a photorefractive optical lattice," New J. Phys. **6**, 47 (2004).

#104257 - $15.00 USD Received 18 Nov 2008; revised 22 Dec 2008; accepted 20 Jan 2009; published 3 Mar 2009

15. T. J. Alexander, A. A. Sukhorukov, and Y. S. Kivshar, "Asymmetric Vortex Solitons in Nonlinear Periodic Lattices," Phys. Rev. Lett. **93**, 063901 (2004).
16. G. A. Swartzlander, Jr., and C. T. Law, "Optical vortex solitons observed in Kerr nonlinear media," Phys. Rev. Lett. **69**, 2503-2506 (1992).
17. V. Tikhonenko and N. Akhmediev, "Excitation of vortex solitons in a Gaussian beam configuration," Opt. Commun. **126**, 108 (1996).
18. I. Towers, A. V. Buryak, R. A. Sammut, B. A. Malomed, L. C. Crasovan, and D. Mihalache, "Stability of spinning ring solitons of the cubic-quintic nonlinear Schrödinger equation," Phys. Lett. A **288**, 292 (2001).
19. H. Michinel, J. Campo-Táboas, M. L. Quiroga-Teixeiro, J. R. Salgueiro and R. García-Fernández, "Excitation of stable vortex solitons in nonlinear cubic-quintic materials," J. Opt. B: Quantum Semiclass. Opt. **3**, 314-317 (2001).
20. H. Michinel, J. R. Salgueiro, and M. J. Paz-Alonso, "Square vortex solitons with a large angular momentum," Phys. Rev. E **70**, 066605 (2004).
21. S. V. Fedorov, N. Rosanov, A. N. Shatsev, N. A. Veretenov, and A. G. Vladimirov, "Topologically multicharged and multihumped rotating solitons in wide-aperture lasers with a saturable absorber," IEEE J. Quantum Electron. **39**, 197 (2003).
22. N. N. Rosanov, "Solitons in laser systems with saturable absorption," in: Dissipative solitons, (Eds.) N. Akhmediev and A. Ankiewicz, Lecture Notes in Physics, V. 661, Springer, Heidelberg, 2005.
23. L.-C. Crasovan, B. A. Malomed and D. Mihalache, "Stable vortex solitons in the two-dimensional Ginzburg-Landau equation," Phys. Rev. E **63**, 016605 (2001).
24. D. Mihalache, D. Mazilu, F. Lederer, H. Leblond and B. A. Malomed. "Collisions between coaxial vortex solitons in the three-dimensional cubic-quintic complex Ginzburg-Landau equation," Phys. Rev. A **77**, 033817 (2008).
25. J. M. Soto-Crespo, D. R. Heatley, E. M. Wright and N. Akhmediev, "Stability of the higher-bound states in a saturable self-focusing medium," Phys. Rev. A **44**, 636-644 (1991).
26. A. Ankiewicz, N. Devine, N. Akhmediev and J. M. Soto-Crespo "Continuously self-focusing and continuously self-defocusing 2-D beams in dissipative media," Phys. Rev. A **77**, 033840 (2008).
27. N. Akhmediev. J. M. Soto-Crespo, and G. Town, "Pulsating solitons, chaotic solitons, period doubling, and pulse coexistence in mode-locked lasers: Complex Ginzburg - Landau equation approach," Phys. Rev. E **63**, 056602 (2001).

1. Introduction

Vortices are screw wave front defects that appear in many branches of physics [1, 2, 3]. In recent years, they attracted much attention in optics [4]. Optical vortices in nonlinear media have special properties and they have been dubbed vortex solitons [5, 6, 7, 8]. They can exist both in continuous [9, 10, 11] and periodic media [12, 13, 14, 15]. Vortices can be located on a plane wave which requires an infinite energy to support them. In reality, most of the studies were restricted to optical vortices that are nested in bright beams [16, 17]. The requirement of zero field at the center of the beam converts them into ring structures. These can exist as exact solutions of nonlinear wave equations. Vortex ring solitons with high value of vorticity are of special interest [18]. Their stability in conservative media is a controversial issue [19, 20]. Generally, ring structures in conservative media have been found to be unstable in respect to the modulation instability [25]. The result of such instability is usually the filamentation of the beam. In this respect, we should note that the stability properties of vortex solitons in dissipative media [21, 22, 23, 24] are quite different from those in conservative media. Thus, dissipative soliton structures require separate studies.

In this paper, we deal with (2+1)-D vortex ring solitons of the cubic-quintic complex Ginzburg-Landau equation (CGLE). Our major observation is that there is a multiplicity of them. We have found families of ring solitons with arbitrary vorticity, (m), including higher-order ones ($m > 2$). For each m, there is a variety of such solutions with the ground state being a stable ring with azimuthal symmetry. The radius of the ring grows with increasing m. They are stable and stationary in large regions of the parameter space. Other types of solutions with the same m bifurcate from the ground state branch at certain values of the parameters. When the vortex ring solitons lose their cylindrical symmetry, they become modulated and exhibit a number of amplitude maxima along the ring. This number is usually equal to the value of the

#104257 - $15.00 USD Received 18 Nov 2008; revised 22 Dec 2008; accepted 20 Jan 2009; published 3 Mar 2009

vorticity plus one, i.e. $m+1$. Generally speaking, vortex solitons without cylindrical symmetry exist in narrower regions of the parameter space and their shapes vary. They remain as a complete ring but acquire a nontrivial azimuthal structure. The ring itself may pulsate and rotate simultaneously or can be involved in only one of these motions. The dynamics of the highest complexity is a chaotic one.

The paper is organized as follows. Section 2 describes the nonlinear dynamical system under study while the following sections present numerical results for the ring solitons with vorticity $m = 1, 2, 3$ and 4 respectively. Each case can be considered as special, because the bifurcation diagram for each m is different. The cases of higher vorticity are treated in the Section 7. Finally, Section 8 summarizes our results.

2. Statement of the problem

Our present study is based on an extended complex Ginzburg-Landau equation [26], that includes cubic and quintic nonlinear terms. In normalized form, this propagation equation reads:

$$i\psi_z + \frac{D}{2}\nabla_\perp^2\psi + |\psi|^2\psi + \nu|\psi|^4\psi = i\delta\psi + i\varepsilon|\psi|^2\psi + i\beta\nabla_\perp^2\psi + i\mu|\psi|^4\psi. \tag{1}$$

where $\psi = \psi(x,y,z)$ is the normalized envelope of the field,

$$\nabla_\perp^2 = \frac{\partial^2}{\partial x^2} + \frac{\partial^2}{\partial y^2}$$

is the two-dimensional transverse Laplacian, z is the propagation distance, (x,y) are the transverse co-ordinates, D is the diffraction coefficient that without loss of generality can be set to 1, ν is the saturation coefficient of the Kerr nonlinearity, δ represents linear losses, ε is the nonlinear gain coefficient, β stands for angular spectral filtering in the medium, and μ characterizes the saturation of the nonlinear gain.

The main parameter of the solution that we calculate in simulations is the beam power, Q:

$$Q(z) = \int_{-\infty}^{\infty}\int_{-\infty}^{\infty}|\psi(x,y,z)|^2 dxdy, \tag{2}$$

The value of Q for a localized solution is finite and changes smoothly while the solution stays within the region of existence of a certain type of solitons. The value of Q changes abruptly when there is a bifurcation and the solution jumps from a branch of solitons that become unstable to another branch of stable solitons. Thus, monitoring Q allows us to find bifurcations in an easy way. Observing a finite Q also reveals the stability of a solution. As soon as the solution becomes unstable, it diverges and the value of Q either converges to another fixed value, vanishes or goes to infinity. In the case that the resulting solution is pulsating, instead of a fixed value of Q, we obtain a band of Q values that corresponds to the changing power of the soliton. Thus, monitoring the power, Q, provides us with essential information about soliton solutions.

Localized structures with vorticity can be created using initial conditions with rotating phase. Additionally, to generate predominantly radially symmetric structures, the initial conditions must also have radial symmetry. We used the following initial condition that satisfy the above criteria:

$$\psi(x,y,0) = A_o r^m \exp\left(-\frac{r^2}{w^2} + im\theta\right) \tag{3}$$

where $r = \sqrt{x^2+y^2}$, m is the vorticity, $\theta = \arctan(y/x)$, w is an approximate radius of the ring structure to be created, and A_o is a real amplitude that should generate sufficient power to place the initial condition into a basin of attraction of a ring vortex soliton. The initial condition

#104257 - $15.00 USD Received 18 Nov 2008; revised 22 Dec 2008; accepted 20 Jan 2009; published 3 Mar 2009

converges to the solution which is stable at the chosen parameters of the equation. In cases when there are two or more stable solutions simultaneously, we have to take additional care choosing the parameters of the initial condition such that it falls into the desired basin of attraction. Once a soliton solution is found for a given set of equation parameters, we use it as initial condition for a nearby set of parameters. This technique is the main tool when looking for the continuous range of existence of solitons of the same type. A random perturbation can be added to stimulate the development of any asymmetry if the stationary solution has one. Numerical noise can also stimulate the asymmetry of the solution. However, the actual convergence to the stable solution in this instance takes longer distances z.

We started our simulations finding only radially symmetric solutions. Usually these solutions occupy finite, relatively large regions in the parameter space. Solutions with different values of m may exist simultaneously at the same set of the equation parameters. Moreover, the regions of existence of vortex solitons with different m roughly coincide. Only the edges of these regions vary slightly with the value of m. This can be seen from Fig. 1 which shows the power, Q, versus ε for radially-symmetric vortex solutions of different vorticity. The set of parameters used in these simulations are shown inside the figure. For a given ε value, the power Q of these solutions is proportional to m with high accuracy, i.e. the solution with vorticity $m > 1$ has virtually m times the power of the vortex soliton with $m = 1$. The examples for values of m from 1 to 5 allow us to conclude that ring vortex solitons with m higher than 5 must also exist. At higher values of m, the solutions are gradually transformed into round stripes of finite width. Thus, at higher m, their stability is related to the stability of the stripe. This means that ring vortex solitons can exist for any higher m value.

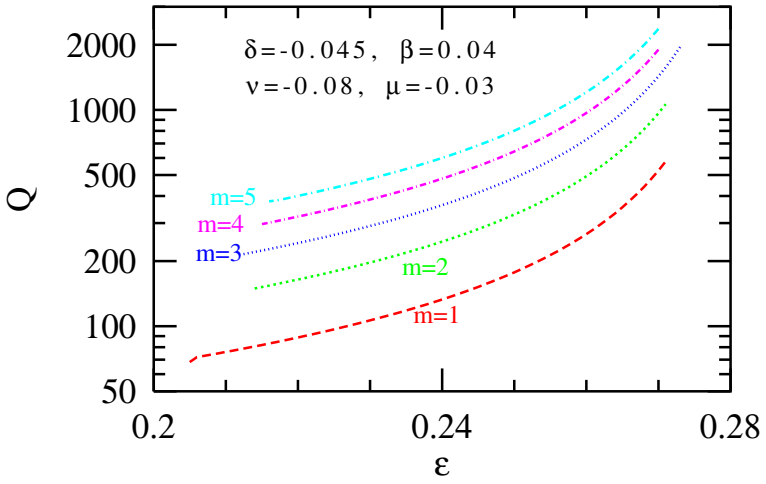

Fig. 1. The power Q vs ε for the radially symmetric vortex dissipative solitons with $m = 1, 2, 3, 4$ and 5. Note the logarithmic scale along the vertical axis.

The region of existence for ring vortex solitons is relatively large in every direction in the parameter space. Even if the parameters are moved well away from those given in Fig. 1, the curves have similar width in ε domain. In the rest of this paper, we use the set of parameters $(\delta, \beta, \mu, \nu)$ to be $(-0.1, 0.1, -0.04, -0.02)$ and change only ε to observe the bifurcations. For this set of parameters, radially symmetric solutions with any particular m also exist in a finite range of ε values. Beyond that range we can observe other types of solutions. These include solutions with broken radial symmetry and non-stationary localized rings. They can be found when, starting from a symmetric vortex solution, we continuously change one of the equation

#104257 - $15.00 USD Received 18 Nov 2008; revised 22 Dec 2008; accepted 20 Jan 2009; published 3 Mar 2009

parameters fixing all the others. At a point of bifurcation, the radially symmetric solution ceases to be stable, and a qualitatively new type of solution appears. The transformations and their location in the parameter space depend very much on the value of m. Therefore, in what follows, we consider separately the bifurcation diagrams for each m.

3. Ring vortex solitons with $m = 1$

Using the set of parameters given in the previous section, we have found a variety of stable ring solitons with vorticity $m = 1$ and the ranges of their existence in the ε domain. These ranges are presented in Fig. 2 with the color curves in the $Q(\varepsilon)$ diagram. Different colors indicate different types of solution. Namely, vortex solutions that are represented by the red curve are radially symmetric, while the blue and green curves represent vortex solitons with broken radial symmetry. In particular, the green dashed curve corresponds to unstable stationary solutions, the green solid line stands for stable stationary ones, and the blue stripe represents stable pulsating ring structures. The finite width of this stripe shows the range of Q-values that the soliton takes in its oscillations.

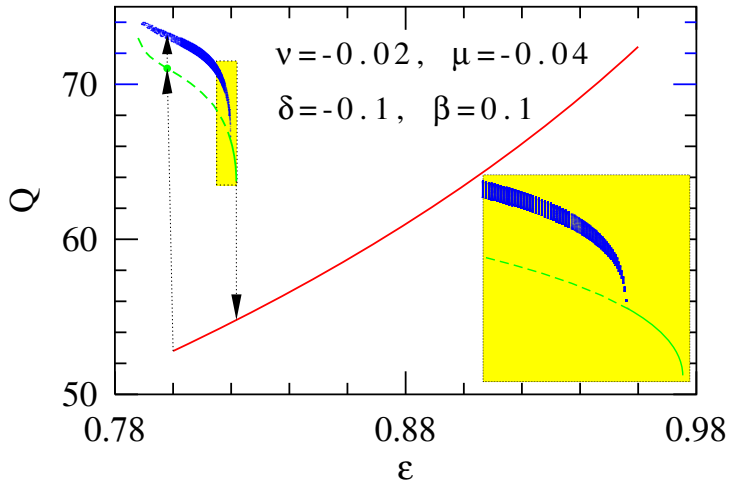

Fig. 2. Power Q versus ε diagram for the ring solitons with vorticity $m = 1$. The red and blue curves and the solid part of the green curve correspond to stable solutions, while the dashed green one is for unstable ones. Solutions on the red curve have a radially symmetric amplitude profile while other solutions are radially asymmetric. The yellow inset in the lower right corner is a magnification of the curves enclosed into the small yellow rectangle in the upper left part of the main diagram. This magnification shows more clearly the bifurcation of the pulsating vortex solutions (blue stripe) from the stationary radially asymmetric ones (green curve).

In order to plot these curves, we started the numerical simulations at the point $\varepsilon = 0.88$ using the initial conditions (3). From this point, we moved step by step in the directions of decreasing and increasing ε and found new solutions using the solution at the previous point as initial condition for the new point. When ε is decreased below 0.80, the radially symmetric vortex solution loses its stability and transforms itself into a vortex soliton without radial symmetry. This transition is shown by the black vertical arrow pointing at a solid dot on the green dashed curve. Solutions on the dashed part of the green curve occurred to be weakly unstable. They are transformed upon farther propagation into pulsating vortex ring solitons. This transformation is shown by the smaller black arrow above the first one.

#104257 - $15.00 USD Received 18 Nov 2008; revised 22 Dec 2008; accepted 20 Jan 2009; published 3 Mar 2009

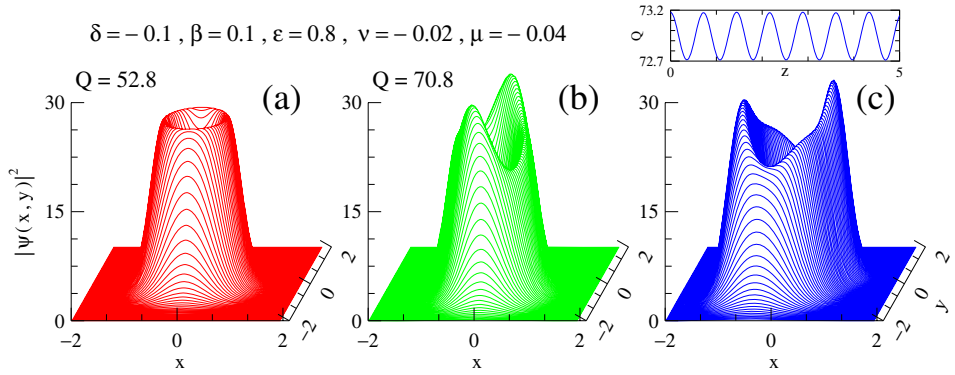

Fig. 3. 2D vortex soliton profiles for $m = 1$ for the equation parameters, written in the upper left part of the figure. In the cases (a) and (b) the power, Q is constant, while for (c) the power is a periodic function of z, as it is shown on top of the panel (c).

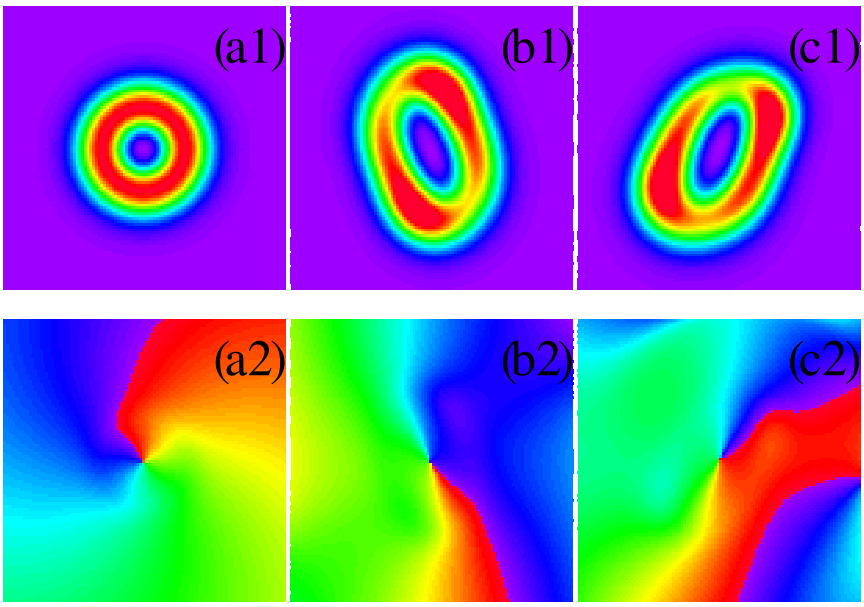

Fig. 4. (Upper row) Contour color plots of the soliton profiles shown in Fig. 3. (Lower row) Contour color plots of the phase profiles for the same solutions. The periodic evolution of the soliton profile shown in (c1) can be seen in the linked movie (Media 1).

Starting the simulations with this new radially asymmetric solution as initial condition, we can plot the $Q(\varepsilon)$ curves for these branches of solitons in the same way as described above, i. e. increasing and decreasing ε in small increments. For clarity, the part of the curves enclosed into the small yellow rectangle in the upper left corner of the diagram is magnified and plotted separately in the lower right hand side yellow panel of Fig. 2. This inset shows clearly the bifurcation of the pulsating solutions from the stationary radially asymmetric ring solitons. The latter solutions turn to be unstable to the left of the point of bifurcation (i. e. on the dashed green line). The instability occurred to be weak and these solutions still can serve as temporary attractors for initial conditions that are close to the radially symmetric solitons of the red curve.

#104257 - $15.00 USD Received 18 Nov 2008; revised 22 Dec 2008; accepted 20 Jan 2009; published 3 Mar 2009

This is why the transition shown by the black arrow stops temporarily at the solid green circle before the solution is further transformed into the pulsating soliton of the blue stripe. Radially asymmetric vortex solitons exist up to the point $\varepsilon = 0.821$. Further increase of ε transforms them into radially symmetric ring solitons. This transition is shown by the black arrow directed down to the red curve. The two arrows enclose the hysteresis cycle.

Soliton profiles in the (x,y) plane for the three types of solutions described above are presented in Fig. 3. The color of the plot corresponds to the color of the curve in Fig. 2 to which they belong. All profiles are calculated for the same set of equation parameters. They are given on the top of the figure. The profile shown in red is radially symmetric while the solutions (b) and (c) are not. The profile in (b) still has two-fold azimuthal symmetry which is lost in further transformations. The two latter solutions rotate on propagation. The profile (c) also changes periodically in z. Consequently, the power Q oscillates as shown in the upper blue panel in (c).

Contour color plots of the same soliton profiles are shown in the upper row of Fig. 4. This plot shows clearly that the solitons of the red branch are radially symmetric while the solitons of the blue and green branches are not. The lower row of Fig. 4 shows the phase contour plots for each solution. In each case, the phase increases by 2π in one rotation around the center of the ring.

Ordinary bell-shaped solitons with zero vorticity also exist at this range of parameters. They are not shown here because the power Q for them is much below the scale of Fig. 2. Namely for the equation parameters presented in Fig. 2, they are stable in the interval of ε values: $[0.30, 0.89]$. This means that if any of the ring vortex solitons loses stability for one or another reason inside the above interval, it will be transformed into a finite number of plain bell-shaped dissipative solitons. The process is similar to a small scale filamentation of the rings [25].

4. Ring solitons with $m = 2$

Following the same procedure as above we have obtained the regions of existence of vortex solitons with $m = 2$ for the same set of parameters as in the previous case. These regions are presented in Fig. 5 by the red and blue curves. In contrast to the case $m = 1$, we have only two branches of ring vortex solitons. The red curve corresponds to solitons with circular symmetry while the radially asymmetric solitons are shown with the blue curve. In each case, the solutions have constant power, Q, at any fixed ε although radially asymmetric solitons may change the shape in propagation. In particular, the solitons represented by the blue curve are close to have a triangular shape with three maxima. In addition, this triangular structure rotates with a constant angular velocity.

An illustrative example of this class of ring vortex solitons is shown in Fig. 6. This example corresponds to the thick filled green circle in Fig. 5. The soliton with $m = 2$ has approximately the same amplitude as the one with $m = 1$ as it is mainly defined by the values of the dissipative parameters δ, ε and μ. However, they occupy a wider space in the (x,y)-plane, thus resulting in the higher values of their power, Q. Another difference from the case $m = 1$ is that the regions of existence in the ε-domain are shifted to smaller values of ε. This is due to the choice of the system parameters which are different from those presented in Fig. 1.

Radially asymmetric solitons on the blue curve are stable. An unstable branch may also exist. It would be natural for this curve to start as a bifurcation at the red curve. However, our numerical technique does not allow us to find these solutions. When changing ε and reaching the right hand side limit of the blue curve, we found a direct transformation of the radially asymmetric ring solitons into the radially symmetric solitons of the red branch. The reverse transformation occurs at the leftmost point of the red curve.

A remarkable feature of the radially asymmetric ring vortex soliton is a three-fold azimuthal bending symmetry along with the specific amplitude modulation. Namely, the number of max-

#104257 - $15.00 USD Received 18 Nov 2008; revised 22 Dec 2008; accepted 20 Jan 2009; published 3 Mar 2009

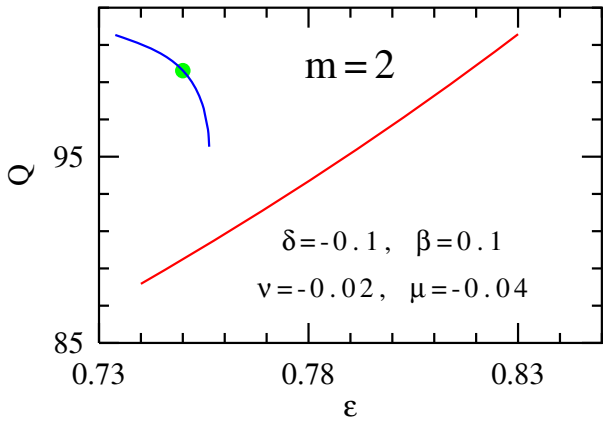

Fig. 5. Regions of existence of vortex solitons with $m = 2$. The red curve corresponds to the radially symmetric ring solitons. Solitons represented by the blue curve are radially asymmetric. The thick filled green circle indicates the location, in the parameter space, of the vortex soliton whose intensity and phase profiles are shown in Fig. 6.

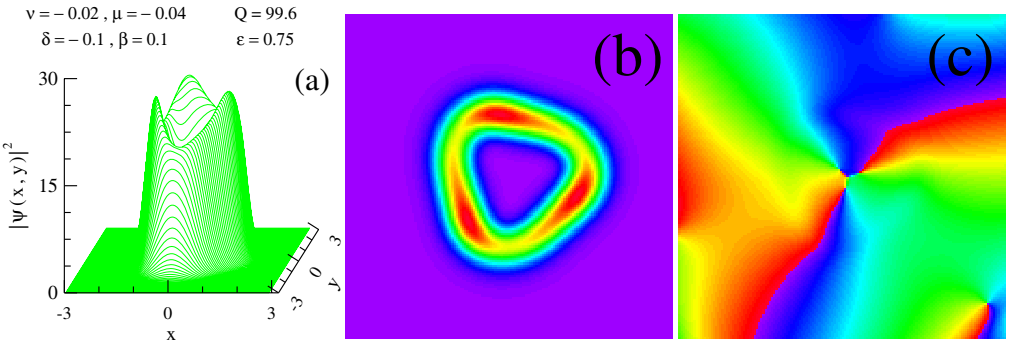

Fig. 6. Radially asymmetric ring vortex soliton with $m = 2$. (a) 3-D plot of the intensity profile. (b) Color contour plot of the same intensity profile in the (x,y)-plane. (c) Color contour plot of the phase profile. The system parameters are chosen at the thick filled green circle in Fig. 5.

ima along the soliton ring is 3 rather than 2. The same type of modulation is observed for radially asymmetric ring solitons with $m = 1$ and $m = 3$. Namely, the number of maxima is equal to $m+1$ (see below for the case $m = 3$). Clearly, the bending symmetry and the amplitude modulation are more related to the length of the ring rather than to its vorticity. In conservative systems, the ring structure can be split into a number of separate beams that depends on the ring diameter [25]. The latter is defined by the growth rate dependence on the spatial frequency of the modulation. In contrast to higher-order beams in conservative media, here, the modulation of the ring dissipative solitons is incomplete, and the ring structure of the soliton does not actually split it into separate beams.

5. Ring solitons with $m = 3$

The regions of existence of ring solitons with $m = 3$ are shown in Fig. 7. Although the radially symmetric ring solitons may have very similar curves for their regions of existence independent of m, their bifurcations into the radially asymmetric ring structures vary significantly with m.

#104257 - $15.00 USD Received 18 Nov 2008; revised 22 Dec 2008; accepted 20 Jan 2009; published 3 Mar 2009

The color notations for the curves in Fig. 7 are the same as in the previous examples. In the case of $m = 3$, the stable radially asymmetric solutions are completely separated in the ε-domain from the stable radially symmetric solutions. Namely, the solid part of the red curve starts when the solid part of the blue curve ends, i.e. the radially symmetric solutions become unstable when the radially asymmetric solutions appear.

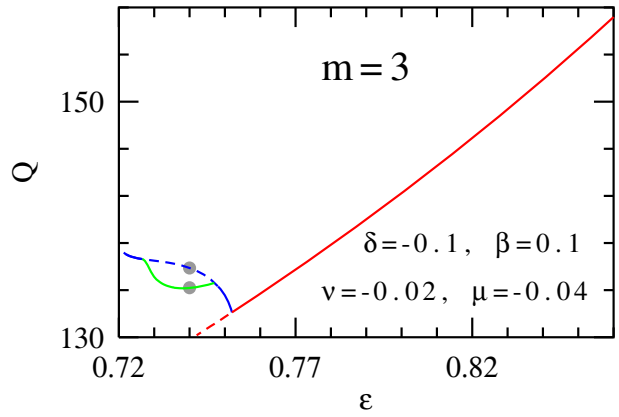

Fig. 7. Regions of existence of vortex solitons with $m = 3$ in the ε domain. The solid (dashed) red curve represents stable (unstable) radially symmetric solitons. The solid blue and green curves correspond to stable radially asymmetric ring solitons while the blue dashed curve stands for unstable ones.

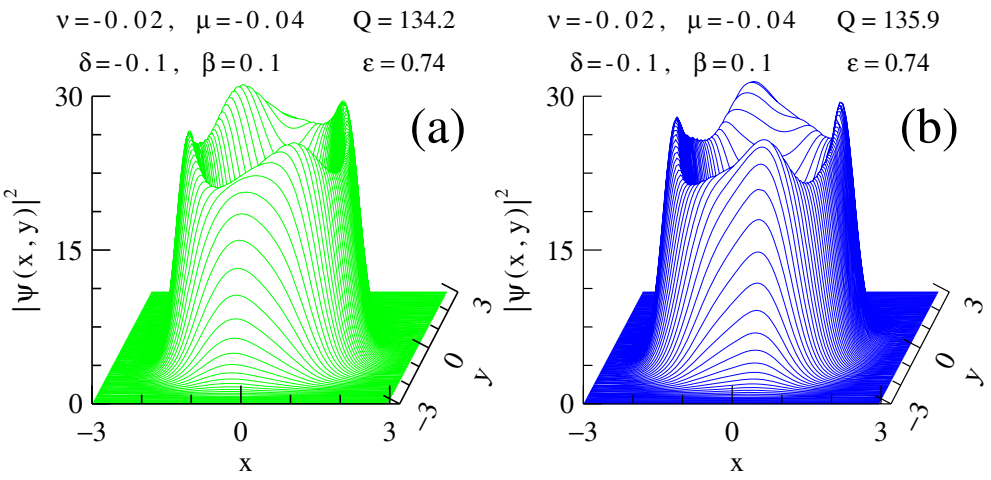

Fig. 8. 3-D intensity profiles of the radially asymmetric ring vortex solutions whose location in the parameter space is indicated in Fig. 7 by the gray filled circles. The two profiles belong to (a) the green and b) the blue branches of solitons in Fig. 7 respectively. The green profile is stable while the blue one is slightly unstable and converges, on propagation, to the green one. The profile (b) has four-fold bending symmetry while the profile in (a) is completely asymmetric. Fig. 9 shows more clearly the difference between them.

All solutions presented in Fig. 7 have fixed power Q at any given ε. We did not find pulsating solitons in the region of ε shown in Fig. 7. The solitons of the branch colored in blue have four-fold bending symmetry. They become unstable when another type of solitons, completely

#104257 - $15.00 USD Received 18 Nov 2008; revised 22 Dec 2008; accepted 20 Jan 2009; published 3 Mar 2009

asymmetric, appear. They are represented by the green branch. In this region, solitons with four-fold bending symmetry are unstable which is shown by a dashed blue line. The growth rate of the instability is small and this allows us to find them using our technique. Two illustrative examples of the solutions with $m = 3$ can be seen in Figs. 8 and 9. Fig. 8 shows the intensity profiles of the two radially asymmetric solutions for $\varepsilon = 0.74$. They are shown in the same color as the corresponding curves in Fig. 7.

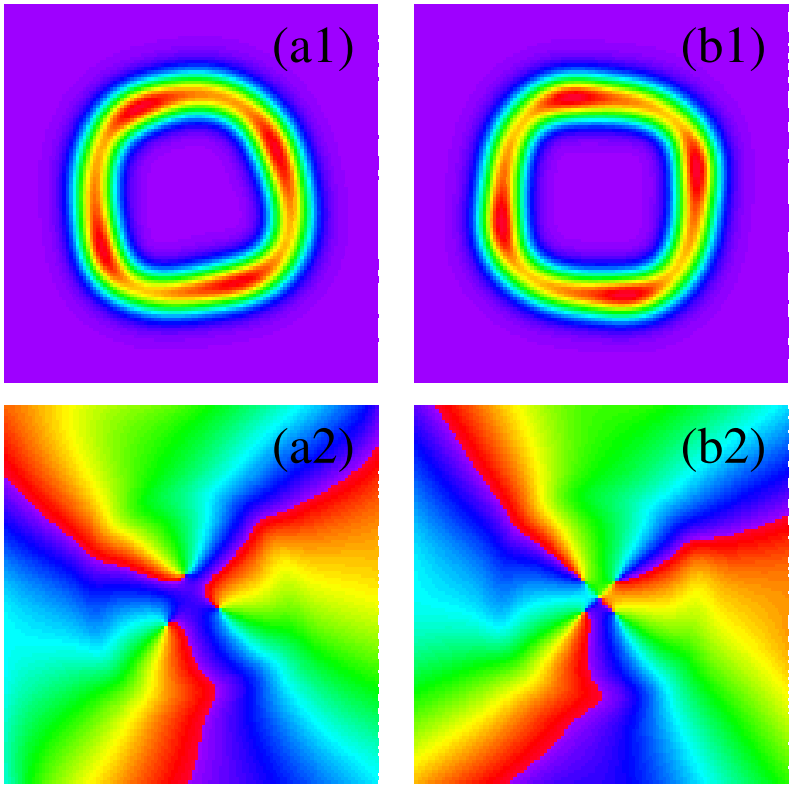

Fig. 9. (upper row) Color contour plots of the intensity in the (x, y) plane of the ring solitons with $m = 3$ shown in Fig. 8. (lower row) Phase profiles for the same solitons. The right column corresponds to the upper grey filled circle in Fig. 7 while the left column to the lower circle. Evolution of each ring soliton can also be seen in animation, i.e. a1) (Media 2) b1) (Media 3).

Each profile is modulated with four maxima and in Fig. 8 they might look similar to each other. The difference can be seen clearly in Fig. 9. While the solution of the blue branch (b1) possess a four-fold azimuthal symmetry having roughly a square shape in the transverse plane, the solution shown in green (a1) does not have that symmetry. The phase profiles corresponding to these solutions are shown in the lower panels of Fig. 9. The evolution of the intensity profiles in these two cases can be seen in the movies associated to the left hand side and right hand side panels in Fig. 9.

6. Ring solitons with $m = 4$

As the vorticity of the ring increases, so does the power of the solutions. This is basically because their diameter becomes larger while the width of the ring is kept essentially constant.

#104257 - $15.00 USD Received 18 Nov 2008; revised 22 Dec 2008; accepted 20 Jan 2009; published 3 Mar 2009

Apart from that, the power versus ε diagrams for radially symmetric solitons look almost similar for all m. However, the transformations to solutions with broken symmetry become more complicated for higher values of m. Thus, the bifurcation diagrams are also becoming more complicated.

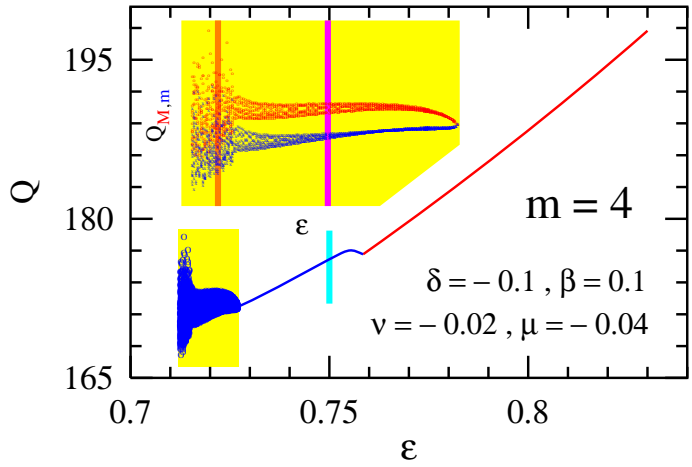

Fig. 10. Bifurcation diagram for the ring vortex solitons with $m = 4$. The upper left yellow inset is a magnified part of the diagram in the lower small yellow box. In the inset, instead or representing the allowed values of Q on propagation, only maxima (red) and minima (blue) of $Q(z)$ are shown

Among the cases $m = 1,2,3,4$, we found the most complex bifurcation diagram for the case $m = 4$. It is shown in Fig. 10. As on the previous diagrams, the red line corresponds to the solutions with radial symmetry. The bifurcation into ring solitons with broken radial symmetry occurs at the edge of this range at $\varepsilon \approx 0.76$. The solid blue line corresponds to stable stationary solitons without radial symmetry. For each ε, they have a fixed value of power Q. These solutions have a pentagonal shape close to the bifurcation point $\varepsilon \approx 0.76$. Five-fold symmetry disappears at lower values of ε and the shape of the solution becomes totally asymmetric. This is illustrated in Fig. 11. While the solution for $\varepsilon = 0.75$ (b), close to the bifurcation point still has approximately a pentagonal shape, the one for $\varepsilon = 0.73$ (a) does not have any particular symmetry. In each case, the ring has 5 intensity maxima.

Bifurcation into pulsating solitons occurs at $\varepsilon \approx 0.727$. This point corresponds to the right hand side limit of the lower little yellow box in Fig. 10. A magnified portion of this part of the bifurcation diagram is shown in the upper yellow inset of Fig. 10. In this inset, instead of representing the allowed values of Q, we show the maxima in red, Q_M, and minima Q_m, in blue, of the function $Q(z)$. These values are taken when they become fixed after the solution has converged to a pulsating soliton and any transitional behavior between the initial conditions and the final state has vanished. Oscillations occur with a single frequency when ε is close to the point of bifurcation. More frequencies appear at lower values of ε, thus resulting in wider stripes for maxima and minima. The motion becomes chaotic at ε around 0.715. Bifurcation into a chaotic pulsation results in two stripes mixed into a single wide band of Q values. In this example, we have a continuous transition into a chaotic state by increasing the number of frequencies involved in the dynamics rather than through a sequence of period doubling bifurcations [27].

In order to show the multi-frequency dynamics of the oscillations of the ring solitons in the region of ε below 0.76, we present some illustrative $Q(z)$ curves in Fig. 12. These curves are

#104257 - $15.00 USD Received 18 Nov 2008; revised 22 Dec 2008; accepted 20 Jan 2009; published 3 Mar 2009

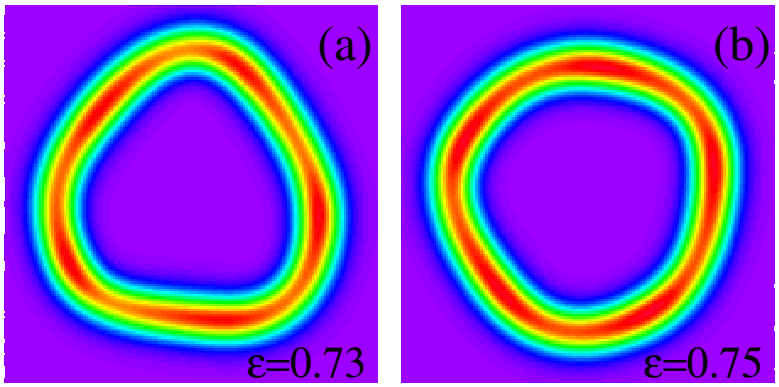

Fig. 11. Two examples of radially asymmetric ring solitons with $m = 4$. Each one can be seen in animation (Media 4 and Media 5).

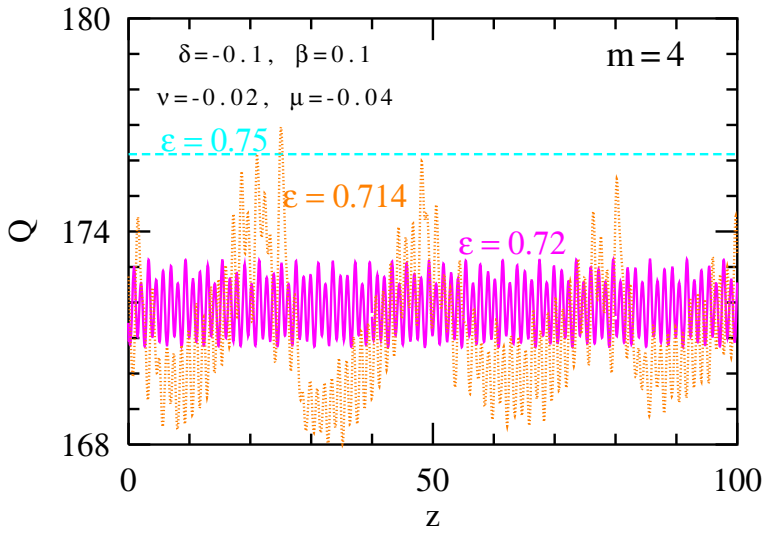

Fig. 12. Evolution of Q for stationary (light blue curve), quasi-periodic pulsating (magenta) and chaotic (orange) vortex solitons. The colors correspond to the thick vertical lines in Fig. 10.

plotted for the values of ε shown by the three vertical colored stripes in Fig. 10 (light blue, magenta and orange). The corresponding curves in Fig. 12 have the same colors. The light blue line with constant Q shows that the ring soliton at this ε has a fixed power despite the fact that the ring soliton has lost its radial symmetry. The curve in magenta shows a multi-frequency dynamics of a pulsating ring soliton. Finally, the orange curve shows a completely chaotic behavior of the solution at $\varepsilon = 0.72$. We should note that there can be intermediate bifurcations where new frequencies are added into the dynamics. However, the density of these bifurcations are high along the ε axis and cannot be well distinguished in our numerical simulations.

7. Ring solitons with $m = 9$

As it can be seen from Fig. 1, ring solitons have a wide range of existence which does not shrink with increasing the vorticity m. This fact allows us to conclude that ring solitons exist for any

#104257 - $15.00 USD Received 18 Nov 2008; revised 22 Dec 2008; accepted 20 Jan 2009; published 3 Mar 2009

higher integer value of m. The fundamental mode always has radial symmetry. The modes which have lower symmetry bifurcate from the fundamental mode. Clearly, in the frame of a single work, we can present only a limited number of examples. Thus, to confirm the existence of ring solitons with higher values of m, we conclude the paper with the case $m = 9$. Firstly, we confirmed that radially symmetric rings do exist in the region of parameters comparable in size with the regions for low values of m. Secondly, we have found the sequence of complicated bifurcations which are not shown here because of the extreme complexity of the bifurcation diagram. Instead, we present just one example of the ring soliton profile. Namely, we have chosen the case, which gained a few new striking features as a result of several bifurcations.

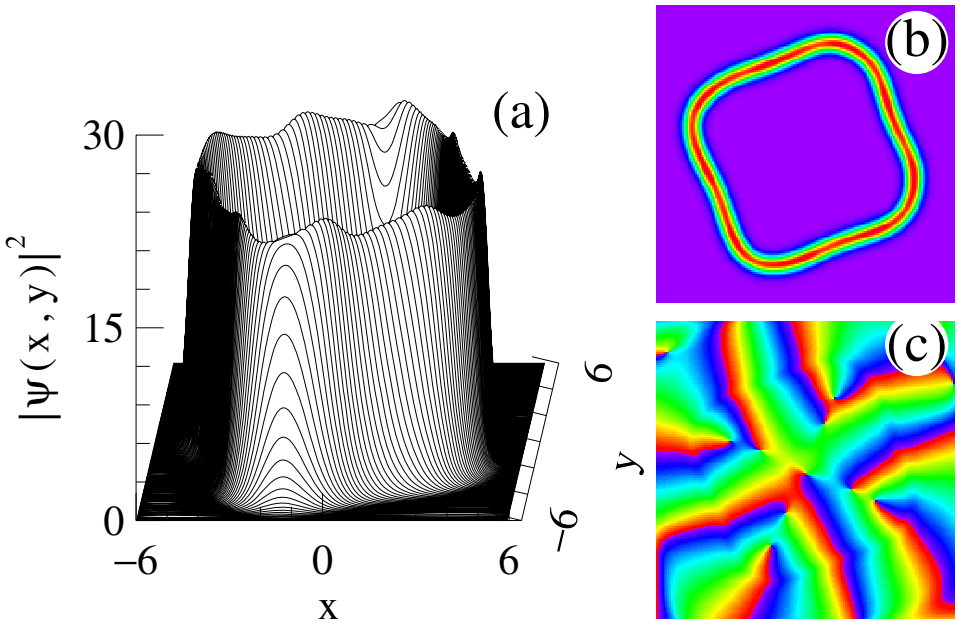

Fig. 13. (a) Three-dimensional plot of the ring soliton with $m = 9$ for $\varepsilon = 0.745$. Color contour plots of (b) the intensity and (c) the phase of the same vortex dissipative soliton.

The first bifurcation is usually related to modulation instability. It creates a modulated structure along the ring with a number of maxima that can coincide with $m+1$ but can also be different from that. In fact, in the case presented here (Fig. 13), the number of maxima does coincide with m. This modulated structure can be seen in Fig. 13(a). Another bifurcation results in the loss of radial symmetry and creates the bending structure. In the case shown in Fig. 13(b), the soliton still has four-fold bending symmetry. This can also be lost in subsequent bifurcations. However, what remains constant in all transformations is the vorticity m. The value $m = 9$ can easily be counted from the phase profile of the soliton in Fig. 13(c).

Subsequent bifurcations add oscillations into the structure, thus forcing the soliton to pulsate. After a set of bifurcations, the ring soliton with $m = 9$ becomes a pulsating solution with two frequencies. These two frequencies are clearly seen in Fig. 14 that shows evolution of Q along z for this pulsating solution. One of them is related to the fast rotation of the modulated structure clockwise around the ring. The lower frequency is related to the rotation of the four-fold azimuthally bended structure in the anti-clockwise direction. Each of these motions can be seen in the movies presented in Fig. 15. The left one corresponds to a short propagation distance, namely z changes from 0 to 6, while in the right one z changes from 0 to 200. In Fig. 15(a), in order to show clearly the motion of the nine maxima along the ring, only the field intensi-

#104257 - $15.00 USD Received 18 Nov 2008; revised 22 Dec 2008; accepted 20 Jan 2009; published 3 Mar 2009

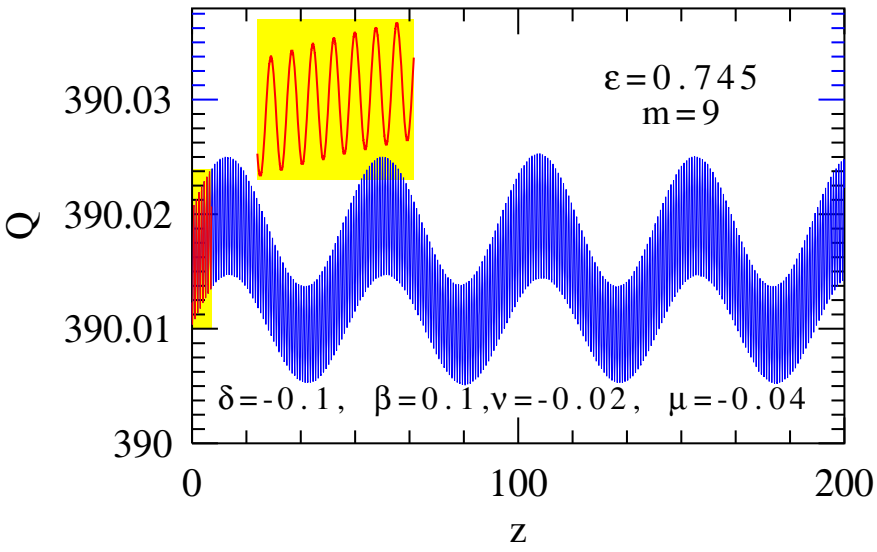

Fig. 14. Double periodic evolution of Q vs z for vortex dissipative soliton with $m = 9$ (blue curve). The yellow inset on the top of the figure shows a magnified part of the blue curve enclosed into a small yellow box to the right of $z = 0$.

ties that exceed the value 0.95 of the absolute maximum of the field intensity are shown. Each of the two frequencies appears as a result of a separate bifurcation similar to those presented in the diagrams for lower values of m. When increasing m however, the complexity of the bifurcation diagrams also increases. Nevertheless, the ring structure is preserved through all the bifurcations. The ring solitons gradually lose higher-order symmetries and become complicated both in shape and in its dynamics. As a final complication, the motion of the ring may become chaotic.

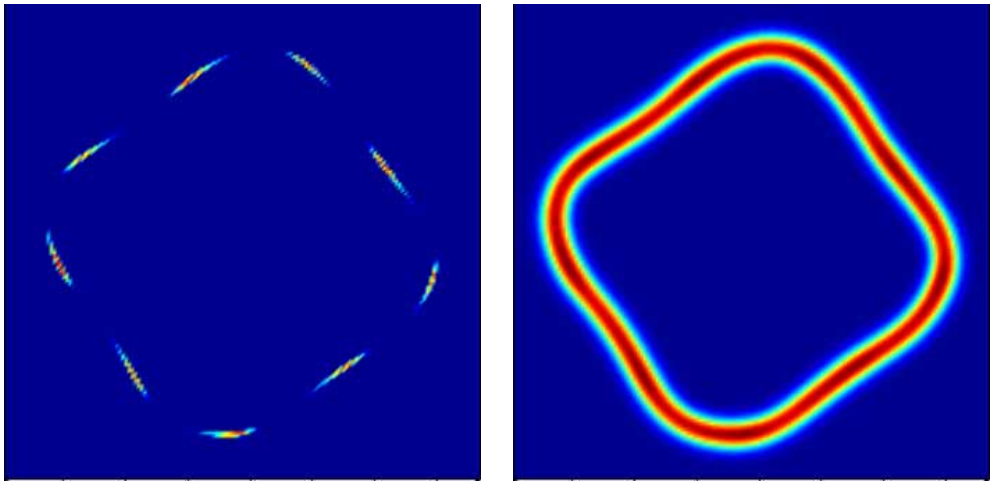

Fig. 15. (a) Movie (Media 6) showing the fast clockwise rotation of the nine maxima of the vortex dissipative soliton with $m = 9$. (b) Movie (Media 7) showing the slow rotation of the dissipative soliton with four-fold bending symmetry in the opposite direction.

#104257 - $15.00 USD Received 18 Nov 2008; revised 22 Dec 2008; accepted 20 Jan 2009; published 3 Mar 2009

These features are characteristic for the ring solitons with values of m higher than 9. The radius of the ring increases with m but the amplitude of the ring stays the same. Thus, the power inside the ring increases roughly linearly with m. There is an infinite number of them but we have to limit ourselves to the lowest order ones. This last case concludes our presentation of the dissipative ring vortex solitons and their properties.

8. Conclusions

In conclusion, we studied (2+1)-D ring vortex structures in dissipative media governed by the complex cubic-quintic Ginzburg-Landau equation. We have found regions of stability for ring solitons with vorticity m ranging from 1 to 5 and additionally for $m = 9$. The existence of vortex ring solitons with m from 1 to 5 and the fact that their region of existence does not shrink when increasing m to 9 shows clearly that such structures can exist for any higher value of m. The unique property of dissipative ring structures is their bifurcation patterns. Radially symmetric ring structures can be transformed into ring structures which are modulated or bent along the ring. They can also pulsate periodically or chaotically. Despite all these transformations, they remain stable as a single ring with given m. These properties make them distinctively different from any known vortex solitons in conservative media.

Acknowledgements

J.M.S.C. and C.M.C. acknowledge support from the M.E.y C. under contract FIS2006-03376. The work of NA and ND is supported by the Australian Research Council (Discovery Project scheme DP0663216).

#104257 - $15.00 USD Received 18 Nov 2008; revised 22 Dec 2008; accepted 20 Jan 2009; published 3 Mar 2009